Supporting information

Anti-EGF receptor aptamer-guided co-delivery of anti-cancer siRNAs and quantum dots for theranosis of triple negative breast cancer

Min Woo Kim[1,2], Hwa Yeon Jeong[1], Seong Jae Kang[1], In Ho Jeong[1], Moon Jung Choi[1], Young Myoung You[1], Chan Su Im[1], In Ho Song[4], Tae Sup Lee[4], Jin Suk Lee[5], Aeju Lee[2,3] and Yong Serk Park[1*]

[1]Department of Biomedical Laboratory Science, Yonsei University, Wonju, Republic of Korea;

[2]International Research Organization for Advance Science and Technology (IROAST), Kumamoto University, Kumamoto, Japan;

[3]Magnesium Research Center, Kumamoto University, Kumamoto, Japan

[4]Division of RI-Convergence Research, Korea Institute of Radiological and Medical Science, Seoul, Republic of Korea;

[5]Department of Anatomy, Yonsei University Wonju Collage of Medicine, Wonju, Republic of Korea;

[*]Corresponding Author: Professor YS Park, Department of Biomedical Laboratory Science, Yonsei University, Wonju, Gangwon 220-710, Republic of Korea

Telephone & Fax: 82-33-760-2448 / 82-33-760-2561

E-mail: parkys@yonsei.ac.kr

Table S1. The vesicular size, ζ-potential, and Q-dot incorporation rate of lipoplexes prepared at varied mole% of DSPE-mPEG$_{2000}$

DSPE-mPEG$_{2000}$/Lipoplexes (mole%)	Vesicle size (nm)	Polydispersity Index (PDI)	ζ-potential (mV)	Q-dot incorporation rate (%)	Q-dot loading capacity (%)
0/100	385 ± 79	0.41 ± 0.36	51.8 ± 1.3	67.9 ± 1.2	11.3 ± 0.2
1/99	339 ± 74	0.32 ± 0.23	22.9 ± 3.1	75.0 ± 6.3	12.5 ± 1.1
4/96	175 ± 5	0.25 ± 0.04	8.0 ± 3.4	94.9 ± 5.8	15.8 ± 0.9
8/92	185 ± 5	0.22 ± 0.03	0.2 ± 0.5	93.7 ± 4.0	15.5 ± 0.7

The values were measured using a Zetasizer Nano-ZS90. Each value indicates the mean ± standard deviation (S.D.) of five measurements.

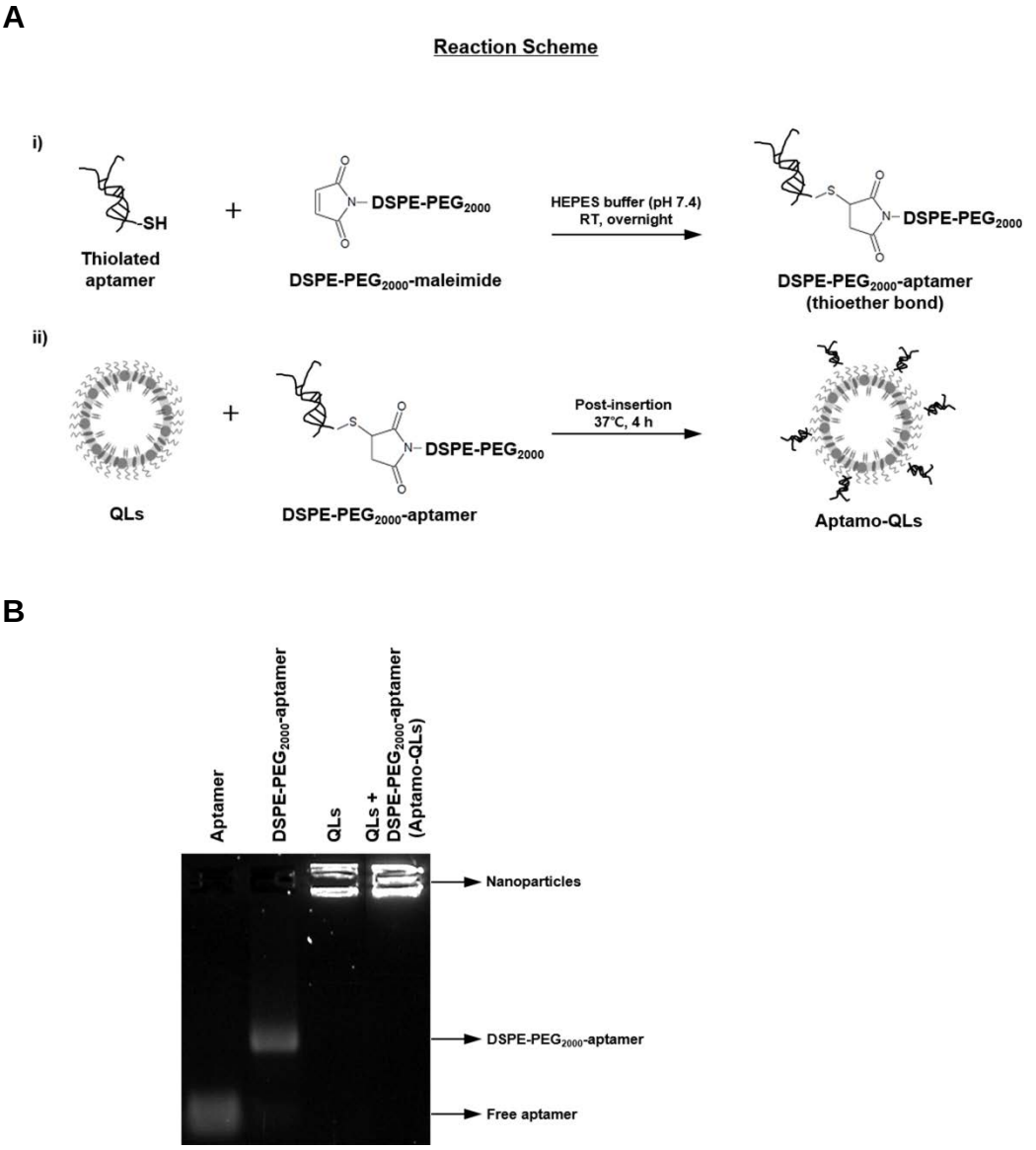

Figure S1. Anti-EGFR aptamer conjugation to DSPE-PEG$_{2000}$-maleimide. (A) Thiolated aptamers were conjugated to DSPE-PEG$_{2000}$-maleimide and post-inserted into QLs. (B) The post-insertion efficiency was measured by electrophoresis using a 1.5% agarose gel. Lane 1: free aptamer, lane 2: DSPE-PEG$_{2000}$-aptamer, lane 3: QLs, and lane 4: QLs inserted with DSPE-PEG$_{2000}$-aptamer.

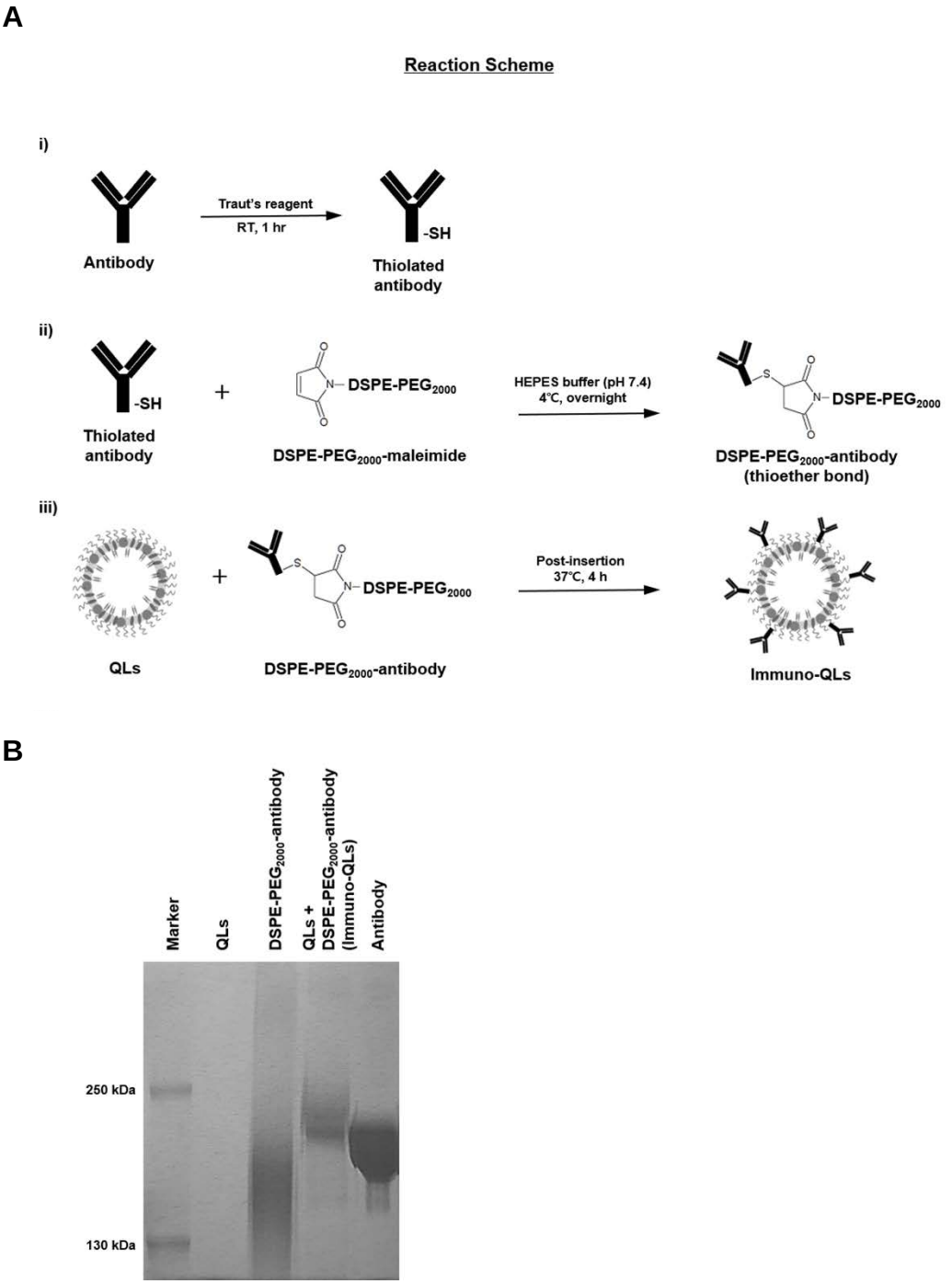

Figure S2. Anti-EGFR antibody conjugation to DSPE-PEG$_{2000}$-maleimide. (A) A procedure of antibody thiolation, antibody conjugation to DSPE-PEG$_{2000}$-maleimide, and insertion of antibody-lipid conjugate into QLs is illustrated. (B) Antibody conjugation to DSPE-PEG$_{2000}$–maleimide and insertion of the conjugate into QLs were verified by 6% SDS-PAGE. Lane 1: marker, lane 2: QLs, lane 3: DSPE-PEG$_{2000}$-antibody, lane 4: DSPE-PEG$_{2000}$-antibody-inserted QLs, and lane 5: free antibody.

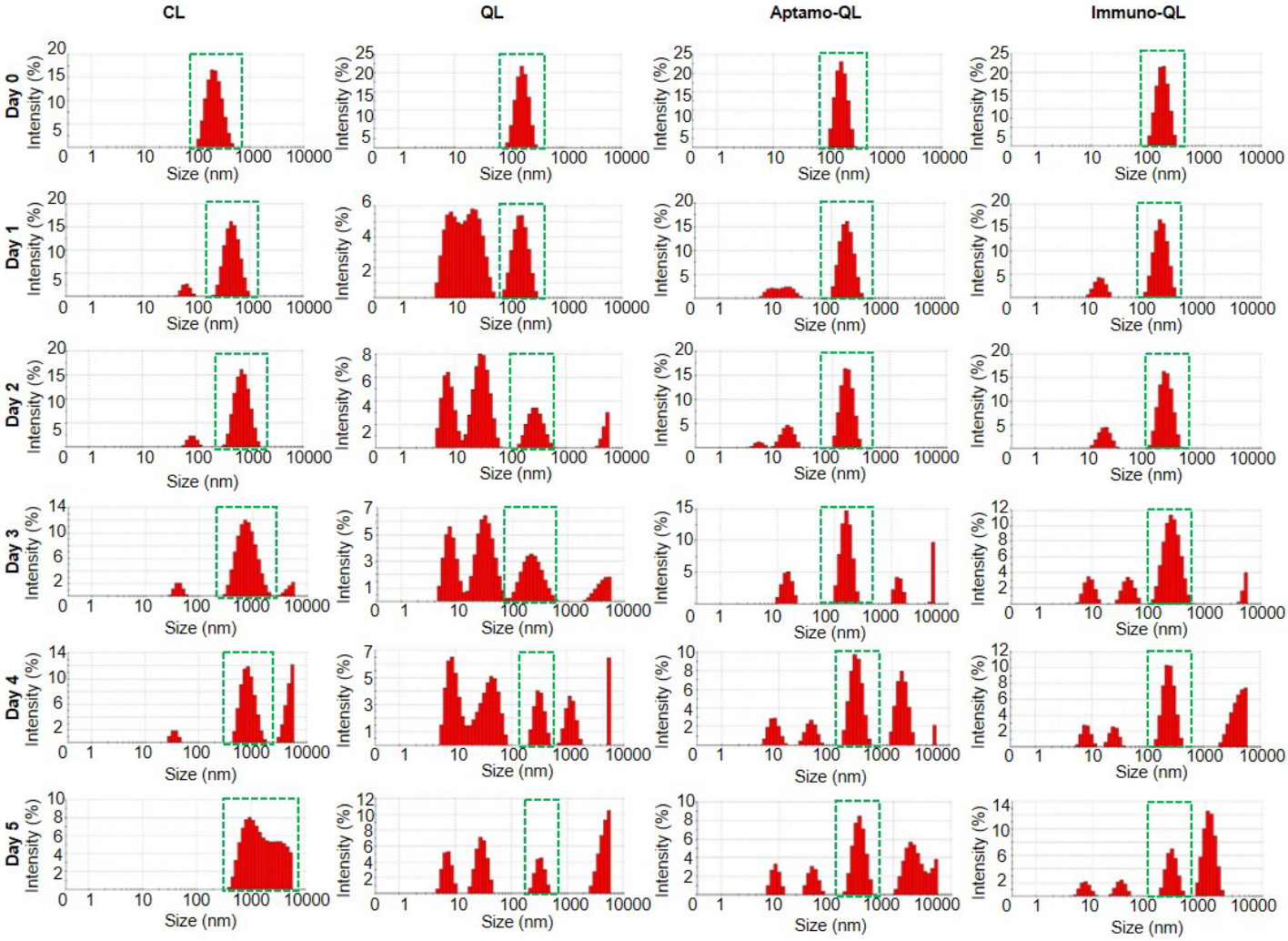

Figure S3. Size changes of aptamo-QLs and immuno-QLs in FBS. The various QL formulations were incubated in the presence of 50% FBS at 37°C and their changes in size were examined with a particle analyzer.

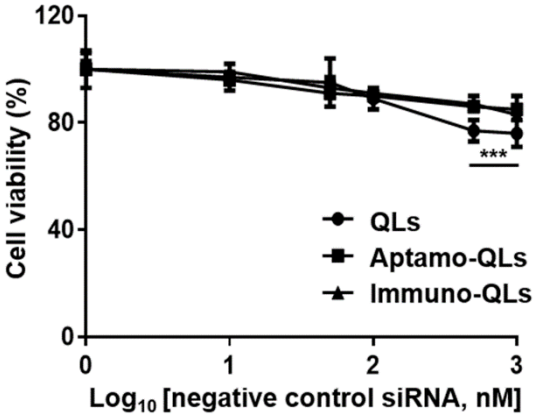

Figure S4. *In vitro* cytotoxicity of aptamo-QLs and immuno-QLs. MDA-MB-231 cells were treated with varied concentrations of prepared negative control siRNA lipoplexes and further cultured for 48 h. Cell viability was measured by the CCK-8 assay. Each error bar represents the mean ± S.D. of five independent experiments. ***$p < 0.001$ vs. untreated control.

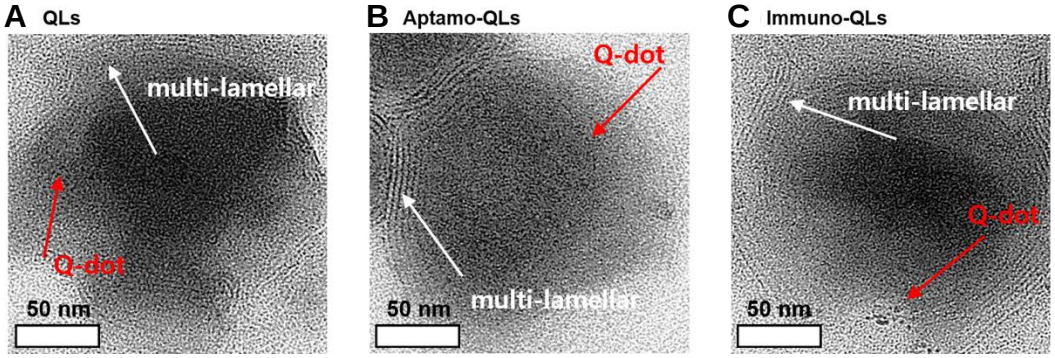

Figure S5. TEM images of aptamo-QLs and immuno-QLs. Representative transmission electron microscopy (TEM) images of QLs (A), aptamo-QLs (B), and immuno-QLs (C) are shown. All lipoplexes showed multi-lamellar structures (white arrow) and Q-dots incorporated in the lipoplex layers (red arrow). Bar = 50 nm.

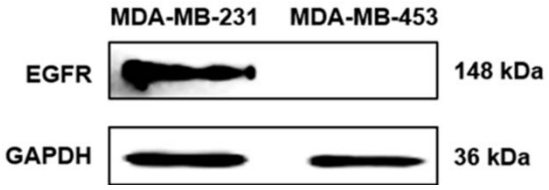

Figure S6. EGFR protein level in MDA-MB-231 and MDA-MB-453 cell lines. Expression of the EGF receptor in MDA-MB-231 and MDA-MB-453 cells was verified by western blotting.

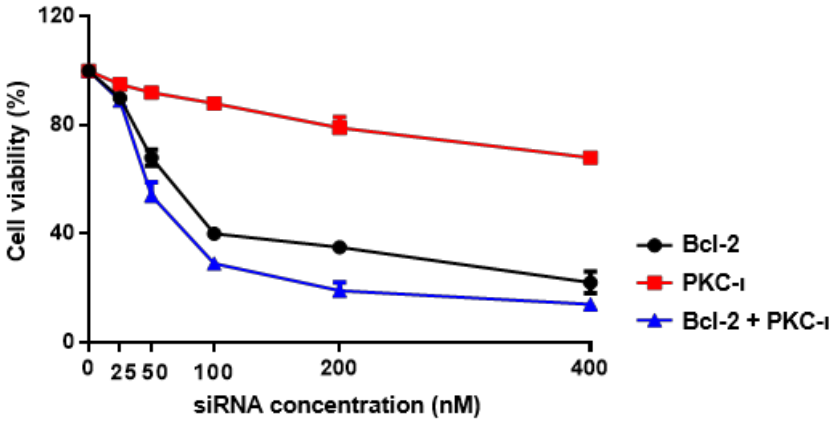

Figure S7. *In vitro* cytotoxicity of Bcl-2 and PKC-ι siRNAs in MDA-MB-231 cells. MDA-MB-231 cells were incubated with QLs encapsulating varied concentrations of Bcl-2 siRNA, PKC-ι siRNA, or Bcl-2/PKC-ι siRNA (1:1 molar ratio) for 48 h. Viability of the transfected cells was measured by the CCK-8 assay.

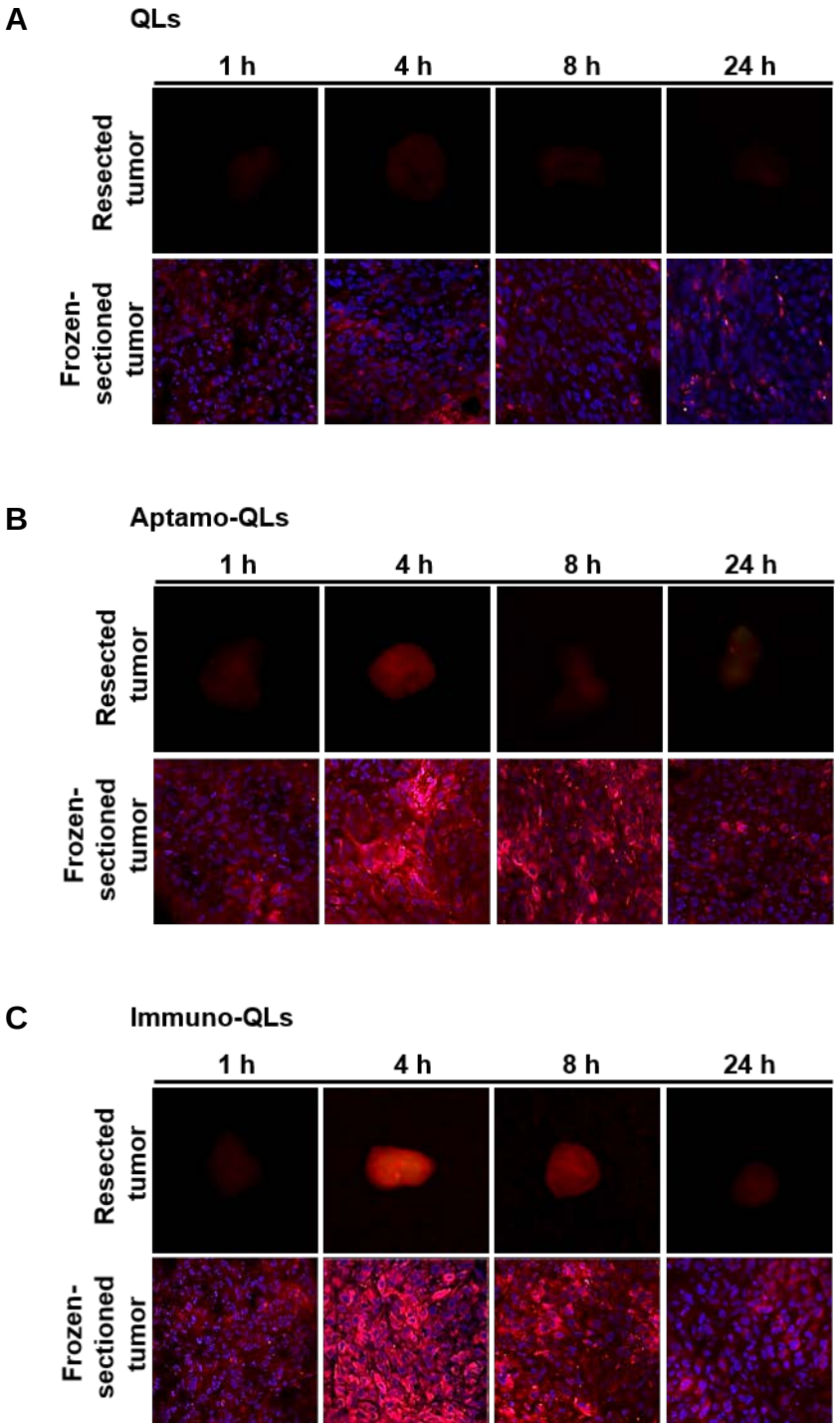

Figure S8. Fluorescence imaging of resected tumors and their frozen-sectioned tissues in mice treated with various QL formulations. After fluorescence imaging, mice intravenously treated with QLs (A), aptamo-QLs (B), and immuno-QLs (C) (0.2 mg lipid/mouse, n = 3) were sacrificed. The fluorescence intensity of resected tumors was observed using the Maestro 2 *in vivo* imaging system, and the frozen-sectioned tumor tissue areas were observed using a confocal microscope at 1, 4, 8, and 24 h time points (×100).

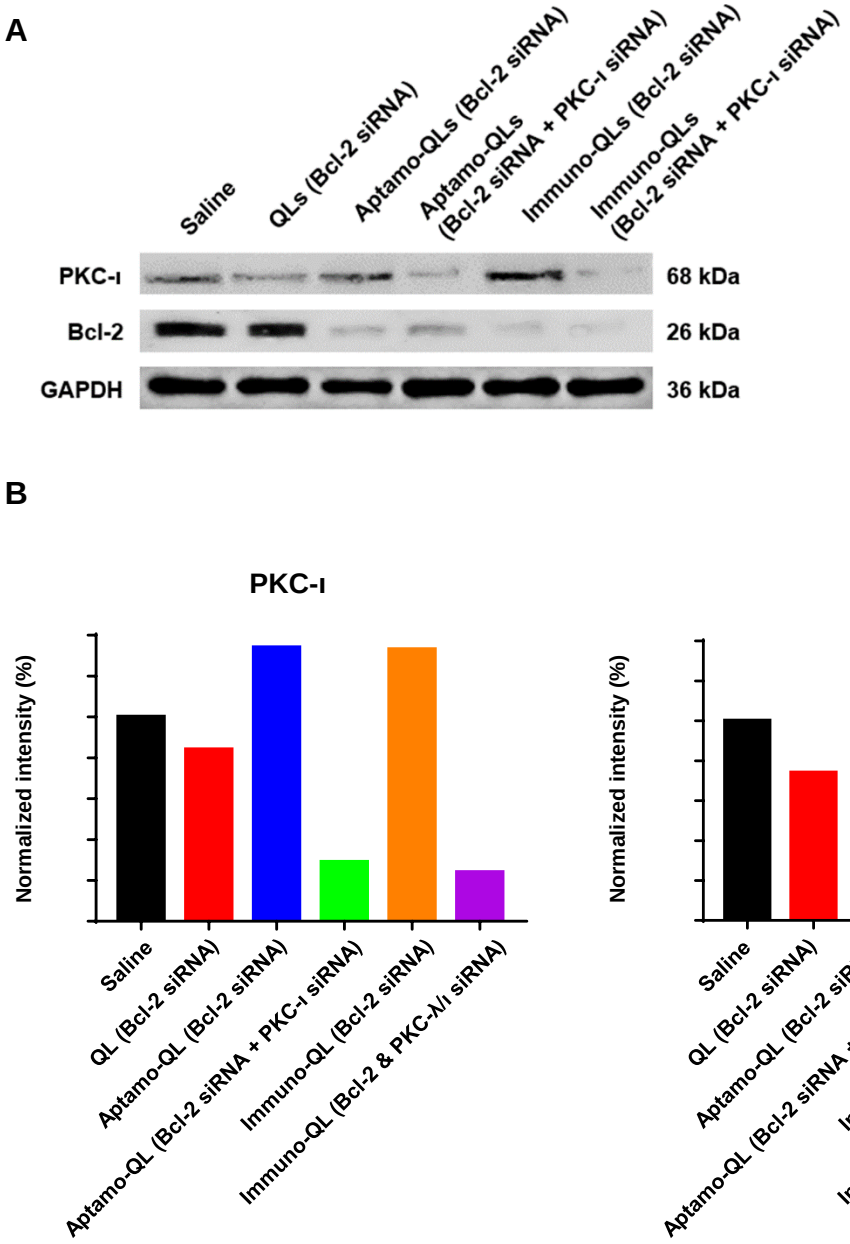

Figure S9. Reduction of Bcl-2 and PKC-ι expression by *in vivo* siRNA transfection.

(A) The tumor-carrying mice were intravenously administered with various QLs encapsulating Bcl-2 and/or PKC-ι siRNAs (10 mg/kg) three times at three-day intervals. At the 10th day post-injection, the mouse tumors were excised, and Bcl-2 and PKC-ι protein expression in the tumors were compared by western blotting analysis (n = 2). (B) The relative band intensities of PKC-ι and Bcl-2 were normalized with GAPDH expression.

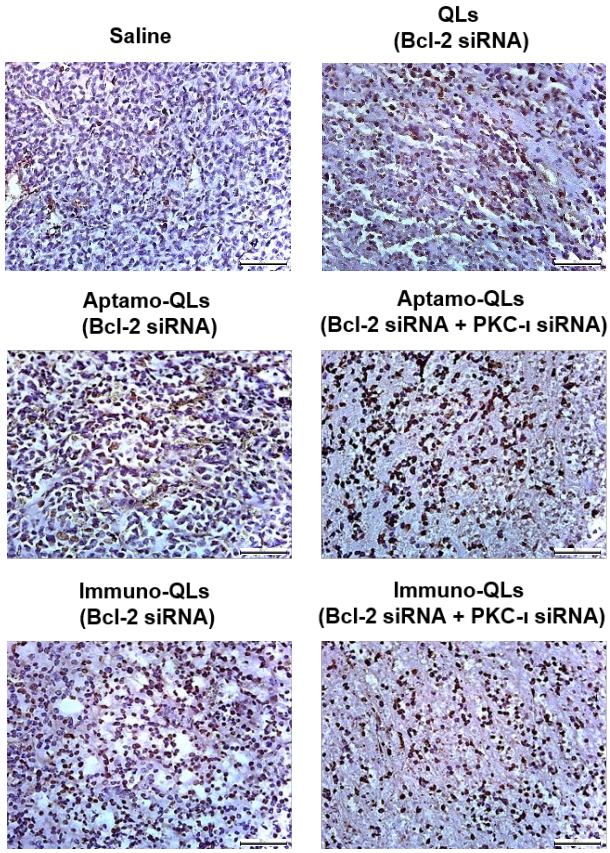

Figure S10. TUNEL staining of tumor sections from mice treated with various QL formulations. TUNEL-positive nuclei in representative tumor sections are shown in brown (n=6). Magnification; ×400. The scale bar is 50 μm long.

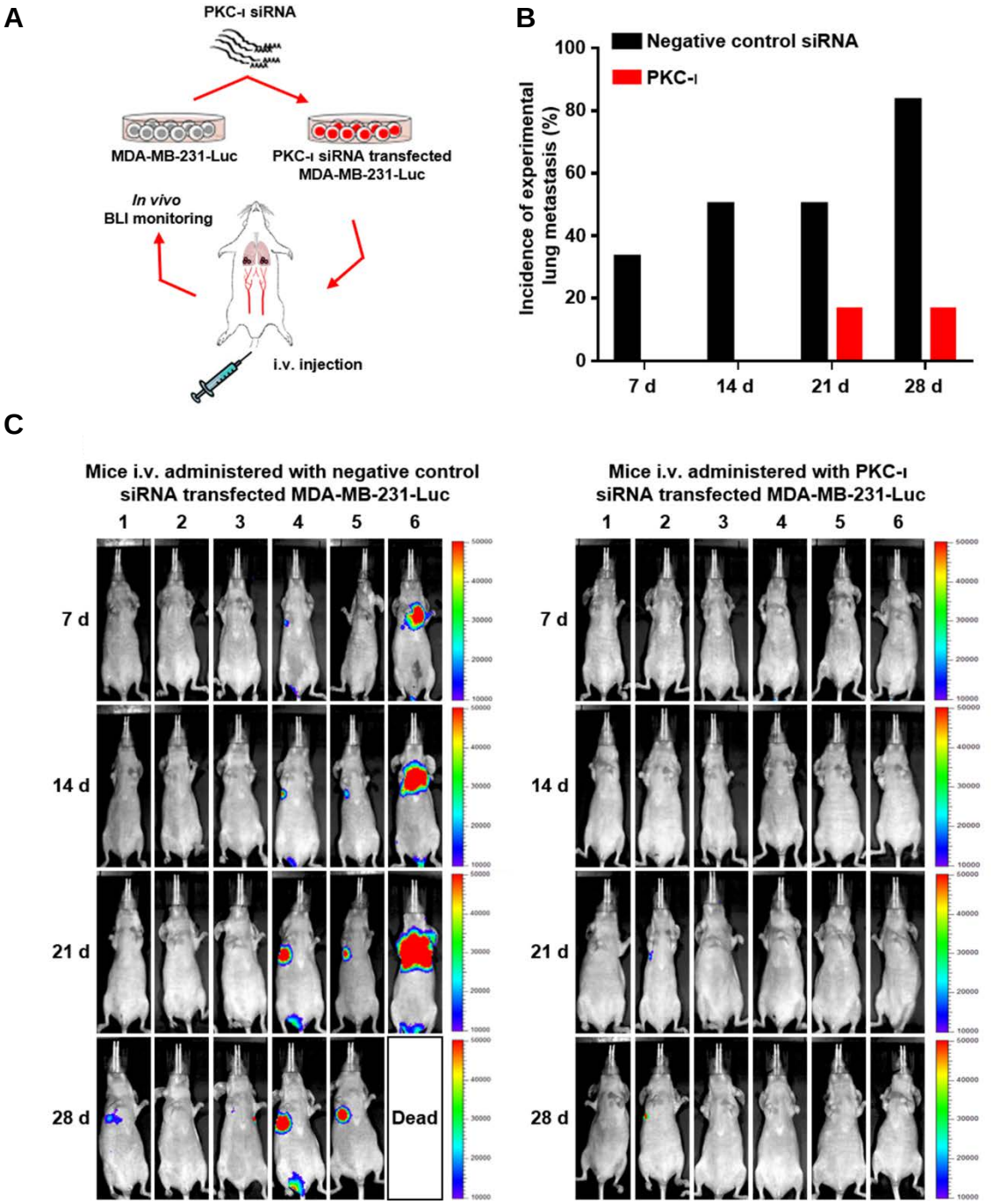

Figure S11. Reduction of pulmonary metastasis by PKC-ι transfection. (A) Schematic of metastatic lung colonization assay after intravenous administration of MDA-MB-231-Luc (2×10^6 cells in 100 μL PBS) with or without PKC-ι transfection. (B) The incidences of experimental lung metastasis were compared in the two groups. (C) The mice intravenously administered with PKC-ι siRNA-transfected MDA-MB-231 cells stably expressing luciferase were monitored by IVIS for 4 weeks using a luciferase assay (n = 6).

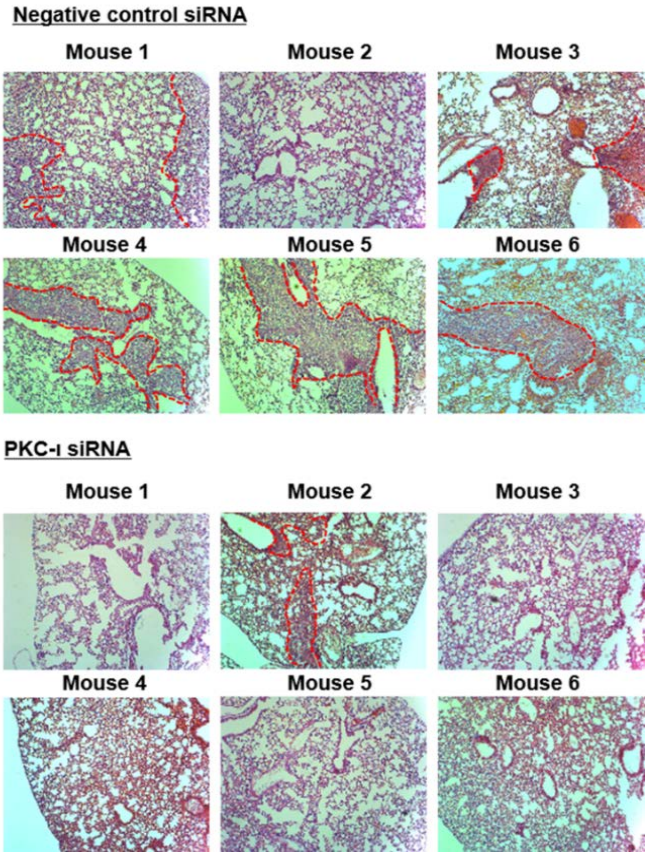

Figure S12. Histological sections of lung tissues from mice intravenously administered with PKC-ι siRNA-transfected MDA-MB-231-Luc. After 4 BLI monitoring by IVIS for 4 weeks using a luciferase assay (n = 6), representative images of lung tissue sections of control (upper) and PKC-ι siRNA-transfected (lower) groups were taken after H&E staining. The tissues in red dotted lines are pulmonary metastasized tumors (×200).

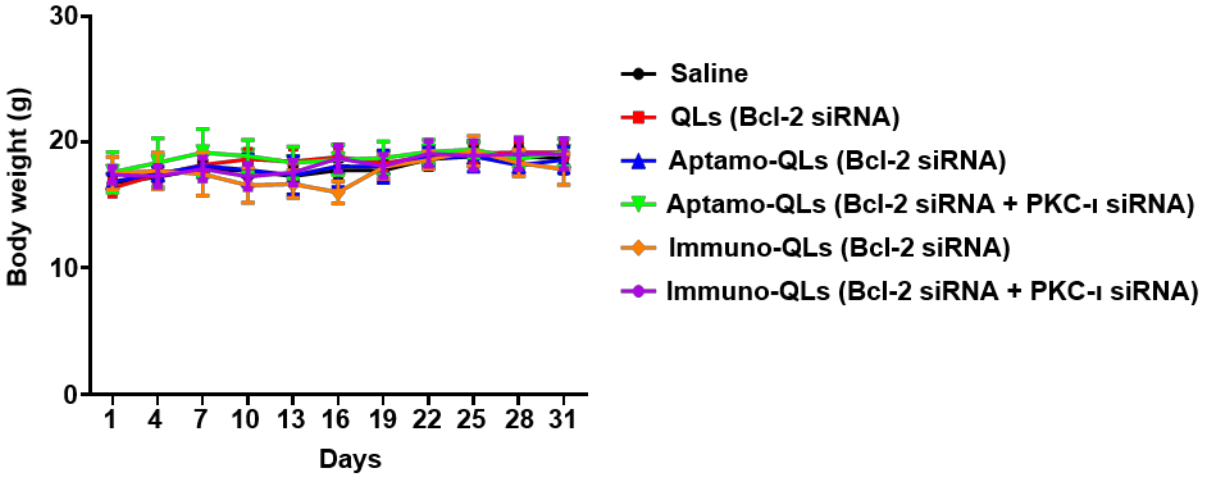

Figure S13. Body weight changes in mice treated with aptamo-QLs and immuno-QLs. Mouse body weights were measured after intravenous administration of the various QLs encapsulating siRNAs (10 mg/kg) three times at three-day intervals (n = 5).

Table S2. Components of lipoplexes

	Components							
						Post-insertion		
	Lipoplex : Q-dots (w/w ratio)	Lipoplex : siRNA (N/P ratio)	DMKE (mole%)	Cholesterol (mole%)	DSPE-mPEG2000 (mole%)	DSPE-mPEG2000 (mole%)	DSPE-PEG2000-Apt (mole%)	DSPE-PEG2000-Ab (mole%)
CLs	-	4:1	50	50	-	-	-	-
QLs	5:1	4:1	48	48	4	-	-	-
Aptamo-QLs	5:1	4:1	46	46	4	3.8	0.2	-
Immuno-QLs	5:1	4:1	46	46	4	3.8	-	0.2